A functional renormalization group approach to zero-dimensional interacting systems

2004 J. Phys.: Condens. Matter 16 5279

(http://iopscience.iop.org/0953-8984/16/29/019)

INSTITUTE OF PHYSICS PUBLISHING JOURNAL OF PHYSICS: CONDENSED MATTER

J. Phys.: Condens. Matter **16** (2004) 5279–5296 PII: S0953-8984(04)80027-4

A functional renormalization group approach to zero-dimensional interacting systems

R Hedden, V Meden, Th Pruschke and K Schönhammer

Institut für Theoretische Physik, Universität Göttingen, Tammannstraße 1, D-37077 Göttingen, Germany

E-mail: meden@theorie.physik.uni-goettingen.de

Received 29 April 2004
Published 9 July 2004
Online at stacks.iop.org/JPhysCM/16/5279
doi:10.1088/0953-8984/16/29/019

Abstract

We apply the functional renormalization group method to the calculation of dynamical properties of zero-dimensional interacting quantum systems. We discuss as case studies the anharmonic oscillator and the single-impurity Anderson model. We truncate the hierarchy of flow equations such that the results are at least correct up to second-order perturbation theory in the coupling. For the anharmonic oscillator, energies and spectra obtained within two different functional renormalization group schemes are compared to numerically exact results, perturbation theory results, and the mean field approximation. Even at large coupling, the results obtained using the functional renormalization group agree quite well with the numerical exact solution. The better of the two schemes is used to calculate spectra of the single-impurity Anderson model, which are then compared to the results from perturbation theory and the numerical renormalization group ones. For small to intermediate couplings the functional renormalization group gives results which are close to the ones obtained using the very accurate numerical renormalization group method. In particular, the low energy scale (Kondo temperature) extracted from the functional renormalization group results shows the expected behaviour.

1. Introduction

The reliable calculation of physical properties of interacting quantum mechanical systems presents a formidable task. Typically, one has to cope with the interplay of different energy scales possibly covering several orders of magnitude even for simple situations. Approximate tools such as perturbation theory, and even numerically exact techniques, can usually handle only a restricted window of energy scales and are furthermore limited in their applicability by the approximations involved or the computational resources available. In addition, due to

the divergence of certain classes of Feynman diagrams some of the interesting many-particle problems cannot be tackled using straightforward perturbation theory.

A general scheme that is designed to handle such a multitude of energy scales and competition of divergences is the renormalization group [1]. The idea of this approach is to start from high energy scales, leaving out possible infrared divergences, and work one's way down to the desired low energy region in a systematic way. The precise definition of the 'systematic way' in general depends on the problem studied.

In particular, for interacting quantum mechanical many-particle systems, two different schemes attempting a unique, problem independent prescription have emerged during the past decade. One is Wegner's flow equation technique [2], where a given Hamiltonian is diagonalized by continuous unitary transformation. From the final result one can extract detailed information about the structure of the ground state and low lying excitations. This technique has been applied successfully to both fermionic and bosonic problems [3]. However, in general it becomes a rather onerous task to really calculate physical quantities, especially dynamics, from correlation functions. Here, one typically has to introduce further approximations [4, 5], again tightly tailored to the problem under investigation.

The second field theoretical approach, which we want to focus on in the following, is based on a functional representation of the partition function of the system under consideration. It has become known as the functional renormalization group (fRG) approach [6–9]. A detailed description of the fRG approach will be given in the next section; here we make some remarks on the principles and discuss previous applications.

Different versions of the fRG approach have been developed over the last few years. One either generates an exact infinite hierarchy of coupled differential equations for the amputated connected m-particle Green functions of the many-body system [6, 9] or generates the one-particle irreducible m-particle vertex functions [7, 8]. For explicit calculations one has to truncate the set of equations, which is the major approximation involved. At what level this truncation is performed to obtain a tractable set of equations depends on the complexity of the problem. Here we exclusively study the one-particle irreducible version of the fRG approach. It has the advantages that it already includes self-energy corrections in low truncation orders and that it can formally easily be extended to higher orders[1].

Up to now, most applications of the fRG approach in many-body physics concentrate on low dimensional, interacting fermion systems where it provides the possibility to sum diverging classes of diagrams. The homogeneous two-dimensional Hubbard model [10–12], the homogeneous one-dimensional Tomonaga–Luttinger model [13], and the one-dimensional lattice model of spinless fermions with nearest neighbour interaction and local impurities [14] were investigated. The focus was on properties of the system close to the Fermi surface, for example on the hierarchy of interactions, for identifying possible instabilities [10–12], or on Tomonaga–Luttinger liquid exponents [13, 14]. The frequency dependence of the vertex functions was mostly neglected[2].

In this paper we investigate the frequency dependence of the self-energy and the effective interaction. For this purpose, we study two different zero-dimensional (local) models: the quantum anharmonic oscillator and a well known problem of solid state physics, the single-impurity Anderson model (SIAM). The former has quite often been used as a 'toy model' for investigating the performance of different approximation schemes of many-particle

[1] We have studied, as an even simpler 'toy model', the classical anharmonic oscillator. We have also investigated, besides the one-particle irreducible version for this model, the fRG schemes using amputated connected Green functions [6] and Wick ordered amputated connected Green functions [9]. Comparing results within the same order of truncation, the irreducible scheme always led to the best results.

[2] Certain aspects of the frequency dependence were taken into account in [13] and [15].

physics [16]. For this problem, conventional perturbation theory is regular—although it generates a generic example of an asymptotic series [16]—and one expects that compared to perturbation theory the fRG approach will lead to a better agreement with the exact solution at larger coupling constants ('renormalization group enhanced perturbation theory'). We calculate the ground state energy and the energy of the first excited state as well as the spectral function of the propagator. Exact results for these observables can be obtained numerically quite easily. The anharmonic oscillator has also been studied using Wegner's flow equation technique [17].

The SIAM has a known hierarchy of energy scales, and presents a true challenge to any many-body tool due to the generation of an exponentially small energy scale, the Kondo scale, leading for example to a sharp resonance in the single-particle spectrum. No exact solutions for dynamical quantities of the model are known. We present fRG results for the one-particle spectral function of the impurity site and compare them to conventional second-order (in the interaction U of the impurity site) perturbation theory results and ones obtained using Wilson's numerical renormalization group (NRG). In both models the truncated fRG scheme, which is correct at least to second-order perturbation theory, leads to a considerable improvement compared to plain second-order perturbation theory.

The paper is organized as follows. In the next section we present a detailed discussion of the fRG approach. The third part contains the application to the quantum anharmonic oscillator, while in the fourth section we discuss the fRG approach for the single-impurity Anderson model. A summary and outlook concludes the paper.

2. The functional renormalization group

Expressed as a functional integral, the grand canonical partition function of a system of quantum mechanical particles (either fermions or bosons) interacting via a two-particle potential can be written as [18]

$$\frac{\mathcal{Z}}{\mathcal{Z}_0} = \frac{1}{\mathcal{Z}_0}\int \mathcal{D}\bar{\psi}\,\psi \exp\left\{(\bar{\psi}, \left[\mathcal{G}^0\right]^{-1}\psi) - S_{\mathrm{int}}\left(\{\bar{\psi}\},\{\psi\}\right)\right\}, \tag{1}$$

with

$$S_{\mathrm{int}}\left(\{\bar{\psi}\},\{\psi\}\right) = \tfrac{1}{4}\sum_{k_1',k_2',k_1,k_2} \bar{v}_{k_1',k_2',k_1,k_2}\bar{\psi}_{k_1'}\bar{\psi}_{k_2'}\psi_{k_2}\psi_{k_1}, \tag{2}$$

$\mathcal{Z}_0$ being the non-interacting partition function. Here ψ and $\bar{\psi}$ denote either Grassmann (fermions) or complex (bosons) fields. The indices $k_j^{(\prime)}$ stand for the quantum numbers of the one-particle basis in which the problem is considered (e.g. momenta and spin directions) and Matsubara frequencies ω. We have introduced the shorthand notation

$$\left(\bar{\psi}, \left[\mathcal{G}^0\right]^{-1}\psi\right) = \sum_{k,k'}\bar{\psi}_k\left[\mathcal{G}^0\right]^{-1}_{k,k'}\psi_{k'},$$

with the propagator $\mathcal{G}^0$ of the related non-interacting problem given as a matrix. The anti-symmetrized (fermions) or symmetrized (bosons) matrix elements of the two-particle interaction are denoted by $\bar{v}_{k_1',k_2',k_1,k_2}$. They contain the energy conserving factor $\delta_{\omega+\omega',\nu+\nu'}$ and the factor $1/\beta$, with $\beta = 1/T$ being the inverse temperature. We consider units such that $\hbar = 1$ and $k_{\mathrm{B}} = 1$. The generating functional of the m-particle Green function is given by

$$\mathcal{W}\left(\{\bar{\eta}\},\{\eta\}\right) = \frac{1}{\mathcal{Z}_0}\int \mathcal{D}\bar{\psi}\,\psi \exp\left\{\left(\bar{\psi}, \left[\mathcal{G}^0\right]^{-1}\psi\right) - S_{\mathrm{int}}(\{\bar{\psi}\},\{\psi\}) - \left(\bar{\psi},\eta\right) - (\bar{\eta},\psi)\right\}, \tag{3}$$

with $(\bar{\psi}, \eta) = \sum_k \bar{\psi}_k \eta_k$ and the external source fields η and $\bar{\eta}$. From this, the generating functional of the connected m-particle Green function follows as

$$\mathcal{W}^{\mathrm{c}}(\{\bar{\eta}\}, \{\eta\}) = \ln[\mathcal{W}(\{\bar{\eta}\}, \{\eta\})]. \tag{4}$$

The (connected) m-particle Green function $G_m^{(\mathrm{c})}$ can be obtained by taking functional derivatives

$$G_m^{(\mathrm{c})}\left(k'_1, \ldots, k'_m; k_1, \ldots, k_m\right) = \frac{\delta^m}{\delta\bar{\eta}_{k'_1} \cdots \delta\bar{\eta}_{k'_m}} \frac{\delta^m}{\delta\eta_{k_m} \cdots \delta\eta_{k_1}} \mathcal{W}^{(\mathrm{c})}(\{\bar{\eta}\}, \{\eta\}) \Big|_{\eta=0=\bar{\eta}}. \tag{5}$$

By a Legendre transformation

$$\Gamma\left(\{\bar{\phi}\}, \{\phi\}\right) = -\mathcal{W}^{\mathrm{c}}(\{\bar{\eta}\}, \{\eta\}) - \left(\bar{\phi}, \eta\right) - (\bar{\eta}, \phi) + \left(\bar{\phi}, [\mathcal{G}^0]^{-1}\phi\right), \tag{6}$$

the generating functional of the one-particle irreducible vertex functions γ_m, with external source fields ϕ and $\bar{\phi}$ and

$$\gamma_m\left(k'_1, \ldots, k'_m; k_1, \ldots, k_m\right) = \frac{\delta^m}{\delta\bar{\phi}_{k'_1} \ldots \delta\bar{\phi}_{k'_m}} \frac{\delta^m}{\delta\phi_{k_m} \ldots \delta\phi_{k_1}} \Gamma\left(\{\bar{\phi}\}, \{\phi\}\right) \Big|_{\phi=0=\bar{\phi}}, \tag{7}$$

is obtained. Note that, in contrast to the usual definition [18] of Γ, ours has an added term $(\bar{\phi}, [\mathcal{G}^0]^{-1}\phi)$ in equation (6) for convenience (see below). The relation between the $G_m^{(\mathrm{c})}$ and γ_m can be found in textbooks [18]. The zero-particle vertex γ_0 provides the interacting part of the grand canonical potential Ω:

$$\Omega = -T \ln \mathcal{Z} = T\gamma_0 - T \ln \mathcal{Z}_0.$$

For the one-particle Green function we obtain

$$G_1(k'; k) = G_1^{\mathrm{c}}(k'; k) = -\zeta \mathcal{G}_{k',k} = \left[\gamma_1 - \zeta[\mathcal{G}^0]^{-1}\right]^{-1}_{k',k},$$

where

$$\mathcal{G}_{k',k} = [[\mathcal{G}^0]^{-1} - \Sigma]^{-1}_{k',k},$$

with the self-energy Σ, and $\zeta = -1$ for fermions and $\zeta = 1$ for bosons, respectively. This implies the relation $\Sigma = \zeta\gamma_1$. The two-particle vertex γ_2 is usually referred to as the effective interaction. For $m \geqslant 3$, the m-particle interaction γ_m has diagrammatic contributions starting at mth order in the two-particle interaction.

In equations (1) and (3) we replace the non-interacting propagator by a propagator $\mathcal{G}^{0,\Lambda}$ depending on a cut-off Λ and $\mathcal{Z}_0$ by $\mathcal{Z}_0^\Lambda$ determined using $\mathcal{G}^{0,\Lambda}$. The boundary conditions for the cut-off $\Lambda \in [\Lambda_0, 0]$ are taken as

$$\mathcal{G}^{0,\Lambda_0} = 0, \qquad \mathcal{G}^{0,\Lambda=0} = \mathcal{G}^0; \tag{8}$$

i.e. at the starting point $\Lambda = \Lambda_0$ no degrees of freedom are 'turned on' while at $\Lambda = 0$ the cut-off independent problem is recovered. In our applications we use a sharp Matsubara frequency cut-off with

$$\mathcal{G}^{0,\Lambda} = \Theta(|\omega| - \Lambda)\,\mathcal{G}^0 \tag{9}$$

and consider $\Lambda_0 \to \infty$ [14]. Through $\mathcal{G}^{0,\Lambda}$, the quantities defined in equations (1)–(7) acquire a Λ dependence. One now derives a functional differential equation for Γ^Λ. From this, by expanding in powers of the external sources, a set of coupled differential equations for γ_m^Λ is obtained.

As a first step we differentiate $\mathcal{W}^{\mathrm{c},\Lambda}$ with respect to Λ, which after straightforward algebra leads to

$$\frac{\mathrm{d}}{\mathrm{d}\Lambda}\mathcal{W}^{\mathrm{c},\Lambda} = \zeta\,\mathrm{Tr}(\mathcal{Q}^\Lambda \mathcal{G}^{0,\Lambda}) + \mathrm{Tr}\left(\mathcal{Q}^\Lambda \frac{\delta^2 \mathcal{W}^{\mathrm{c},\Lambda}}{\delta\bar{\eta}\delta\eta}\right) + \zeta\left(\frac{\delta\mathcal{W}^{\mathrm{c},\Lambda}}{\delta\eta}, \mathcal{Q}^\Lambda \frac{\delta\mathcal{W}^{\mathrm{c},\Lambda}}{\delta\bar{\eta}}\right), \tag{10}$$

with

$$\mathcal{Q}^{\Lambda} = \frac{\mathrm{d}}{\mathrm{d}\Lambda}\left[\mathcal{G}^{0,\Lambda}\right]^{-1}. \tag{11}$$

Considering ϕ and $\bar{\phi}$ as the fundamental variables, we obtain from equation (6)

$$\frac{\mathrm{d}}{\mathrm{d}\Lambda}\Gamma^{\Lambda}\left(\{\bar{\phi}\},\{\phi\}\right) = -\frac{\mathrm{d}}{\mathrm{d}\Lambda}\mathcal{W}^{\mathrm{c},\Lambda}\left(\{\bar{\eta}^{\Lambda}\},\{\eta^{\Lambda}\}\right) - \left(\bar{\phi},\frac{\mathrm{d}}{\mathrm{d}\Lambda}\eta^{\Lambda}\right) - \left(\frac{\mathrm{d}}{\mathrm{d}\Lambda}\bar{\eta}^{\Lambda},\phi\right) + \left(\bar{\phi},\mathcal{Q}^{\Lambda}\phi\right).$$

Applying the chain rule and using equation (10), this leads to

$$\frac{\mathrm{d}}{\mathrm{d}\Lambda}\Gamma^{\Lambda} = -\zeta\,\mathrm{Tr}(\mathcal{Q}^{\Lambda}\mathcal{G}^{0,\Lambda}) - \mathrm{Tr}\left(\mathcal{Q}^{\Lambda}\frac{\delta^2\mathcal{W}^{\mathrm{c},\Lambda}}{\delta\bar{\eta}^{\Lambda}\delta\eta^{\Lambda}}\right).$$

The last term in equation (6) is exactly cancelled, which *a posteriori* justifies its inclusion. Using the well known relation [18] between the second functional derivatives of Γ and $\mathcal{W}^{\mathrm{c}}$ we obtain the functional differential equation

$$\frac{\mathrm{d}}{\mathrm{d}\Lambda}\Gamma^{\Lambda} = -\zeta\,\mathrm{Tr}\big(\mathcal{Q}^{\Lambda}\mathcal{G}^{0,\Lambda}\big) - \mathrm{Tr}\big(\mathcal{Q}^{\Lambda}\mathcal{V}^{1,1}_{\bar{\phi},\phi}(\Gamma^{\Lambda},\mathcal{G}^{0,\Lambda})\big), \tag{12}$$

where $\mathcal{V}^{1,1}_{\bar{\phi},\phi}$ stands for the upper left block of the matrix

$$\mathcal{V}_{\bar{\phi},\phi}(\Gamma^{\Lambda},\mathcal{G}^{\Lambda}) = \begin{pmatrix} \frac{\delta^2\Gamma^{\Lambda}}{\delta\bar{\phi}\delta\phi} - \zeta[\mathcal{G}^{0,\Lambda}]^{-1} & \frac{\delta^2\Gamma^{\Lambda}}{\delta\bar{\phi}\delta\bar{\phi}} \\ \frac{\delta^2\Gamma^{\Lambda}}{\delta\phi\delta\phi} & \frac{\delta^2\Gamma^{\Lambda}}{\delta\phi\delta\bar{\phi}} - [[\mathcal{G}^{0,\Lambda}]^{-1}]^{\mathrm{t}} \end{pmatrix}^{-1} \tag{13}$$

and the superscript t denotes the transposed matrix. To obtain differential equations for the γ_m^{Λ} which include self-energy corrections we express $\mathcal{V}_{\bar{\phi},\phi}$ in terms of $\mathcal{G}^{\Lambda}$ instead of $\mathcal{G}^{\Lambda,0}$. This is achieved by defining

$$\mathcal{U}_{\bar{\phi},\phi} = \frac{\delta^2\Gamma^{\Lambda}}{\delta\bar{\phi}\delta\phi} - \gamma_1^{\Lambda}$$

and using

$$\mathcal{G}^{\Lambda} = [[\mathcal{G}^{0,\Lambda}]^{-1} - \zeta\gamma_1^{\Lambda}]^{-1} \tag{14}$$

which leads to

$$\frac{\mathrm{d}}{\mathrm{d}\Lambda}\Gamma^{\Lambda} = -\zeta\,\mathrm{Tr}\big(\mathcal{Q}^{\Lambda}\mathcal{G}^{0,\Lambda}\big) + \zeta\,\mathrm{Tr}\big(\mathcal{G}^{\Lambda}\mathcal{Q}^{\Lambda}\tilde{\mathcal{V}}^{1,1}_{\bar{\phi},\phi}(\Gamma^{\Lambda},\mathcal{G}^{\Lambda})\big), \tag{15}$$

with

$$\tilde{\mathcal{V}}_{\bar{\phi},\phi}\left(\Gamma^{\Lambda},\mathcal{G}^{\Lambda}\right) = \left[\mathbf{1} - \begin{pmatrix} \zeta\mathcal{G}^{\Lambda} & 0 \\ 0 & [\mathcal{G}^{\Lambda}]^{\mathrm{t}} \end{pmatrix}\begin{pmatrix} \mathcal{U}_{\bar{\phi},\phi} & \frac{\delta^2\Gamma^{\Lambda}}{\delta\bar{\phi}\delta\bar{\phi}} \\ \frac{\delta^2\Gamma^{\Lambda}}{\delta\phi\delta\phi} & \zeta\mathcal{U}^{\mathrm{t}}_{\bar{\phi},\phi} \end{pmatrix}\right]^{-1}. \tag{16}$$

For later applications it is important to note that $\mathcal{U}_{\bar{\phi},\phi}$ as well as $\frac{\delta^2\Gamma^{\Lambda}}{\delta\bar{\phi}\delta\bar{\phi}}$ and $\frac{\delta^2\Gamma^{\Lambda}}{\delta\phi\delta\phi}$ are at least quadratic in the external sources. The initial condition for the exact functional differential equation (15) can be obtained either from lengthy but straightforward algebra, not presented here, or from the following simple argument: at $\Lambda = \Lambda_0$, $\mathcal{G}^{0,\Lambda_0} = 0$ (no degrees of freedom are 'turned on') and in a perturbative expansion of the $\gamma_m^{\Lambda_0}$ the only term which does not vanish is the bare two-particle vertex. We thus find

$$\Gamma^{\Lambda_0}\left(\{\bar{\phi}\},\{\phi\}\right) = S_{\mathrm{int}}\left(\{\bar{\phi}\},\{\phi\}\right). \tag{17}$$

An exact infinite hierarchy of flow equations for the γ_m^{Λ} can be obtained by expanding equation (16) in a geometric series and Γ^{Λ} in the external sources:

$$\Gamma^{\Lambda}\left(\{\bar{\phi}\},\{\phi\}\right) = \sum_{m=0}^{\infty}\frac{\zeta^m}{(m!)^2}\sum_{k'_1,\ldots,k'_m}\sum_{k_1,\ldots,k_m}\gamma_m^{\Lambda}\left(k'_1,\ldots,k'_m;k_1,\ldots,k_m\right)\bar{\phi}_{k'_1}\ldots\bar{\phi}_{k'_m}\phi_{k_m}\ldots\phi_{k_1}.$$

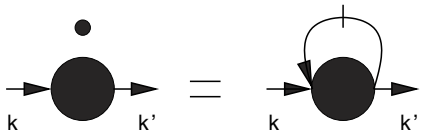

Figure 1. The diagrammatic form of the flow equation for $\gamma_1^\Lambda = \zeta \Sigma^\Lambda$. The slashed line stands for the single-scale propagator $\mathcal{S}^\Lambda$.

The equation for γ_0^Λ reads

$$\frac{\mathrm{d}}{\mathrm{d}\Lambda}\gamma_0^\Lambda = -\zeta \,\mathrm{Tr}\big(\mathcal{Q}^\Lambda \mathcal{G}^{0,\Lambda}\big) + \zeta \,\mathrm{Tr}\big(\mathcal{Q}^\Lambda \mathcal{G}^\Lambda\big). \tag{18}$$

Via $\mathcal{G}^\Lambda$, the derivative of γ_0^Λ couples to the one-particle self-energy. For the flow of the self-energy we obtain

$$\frac{\mathrm{d}}{\mathrm{d}\Lambda}\gamma_1^\Lambda(k';k) = \zeta\frac{\mathrm{d}}{\mathrm{d}\Lambda}\Sigma^\Lambda_{k',k} = \mathrm{Tr}\big(\mathcal{S}^\Lambda \gamma_2^\Lambda(k',\ldots;k,\ldots)\big), \tag{19}$$

with the so-called single-scale propagator

$$\mathcal{S}^\Lambda = \mathcal{G}^\Lambda \mathcal{Q}^\Lambda \mathcal{G}^\Lambda. \tag{20}$$

Here $\gamma_2^\Lambda(k',\ldots;k,\ldots)$ is a matrix in the variables not explicitly written out, i.e. $[\gamma_2^\Lambda(k',\ldots;k,\ldots)]_{q',q} = \gamma_2^\Lambda(k',q';k,q)$. Equation (19) is shown diagrammatically in figure 1. The derivative of γ_1^Λ is determined by γ_1^Λ and the two-particle vertex γ_2^Λ. Thus an equation for γ_2^Λ is required:

$$\begin{aligned}\frac{\mathrm{d}}{\mathrm{d}\Lambda}\gamma_2^\Lambda(k_1',k_2';k_1,k_2) &= \mathrm{Tr}\big(\mathcal{S}^\Lambda\gamma_3^\Lambda(k_1',k_2',\ldots;k_1,k_2,\ldots)\big)\\ &+ \zeta\,\mathrm{Tr}(\mathcal{S}^\Lambda\gamma_2^\Lambda(\ldots,\ldots;k_1,k_2)[\mathcal{G}^\Lambda]^{\mathrm{t}}\gamma_2^\Lambda(k_1',k_2';\ldots,\ldots))\\ &+ \zeta\,\mathrm{Tr}(\mathcal{S}^\Lambda\gamma_2^\Lambda(k_1',\ldots;k_1,\ldots)\mathcal{G}^\Lambda\gamma_2^\Lambda(k_2',\ldots;k_2,\ldots)\\ &+ \zeta[k_1'\leftrightarrow k_2'] + \zeta[k_1\leftrightarrow k_2] + [k_1'\leftrightarrow k_2', k_1\leftrightarrow k_2]).\end{aligned} \tag{21}$$

The corresponding diagrammatic representation is shown in figure 2. The right-hand side (rhs) of equation (21) contains γ_1^Λ, γ_2^Λ, and the three-particle vertex γ_3^Λ. For $m \geqslant 1$ the equation for $\frac{\mathrm{d}}{\mathrm{d}\Lambda}\gamma_m^\Lambda$ contains $\gamma_{m'}^\Lambda$ with $m' = 1, 2, \ldots, m, m+1$. The initial condition for the $\gamma_m^{\Lambda_0}$ can be obtained from equation (17) and is given by

$$\gamma_2^{\Lambda_0}(k_1',k_2';k_1,k_2) = \bar{v}_{k_1',k_2',k_1,k_2}, \qquad \gamma_m^{\Lambda_0} = 0 \qquad \text{for } m \neq 2. \tag{22}$$

We here refrain from explicitly presenting equations for $\frac{\mathrm{d}}{\mathrm{d}\Lambda}\gamma_m^\Lambda$ with $m \geqslant 3$ since later on the set of differential equations is truncated by setting $\gamma_3^\Lambda = \gamma_3^{\Lambda_0} = 0$, which implies that vertices with $m \geqslant 3$ do not contribute.

Following the above systematics, a truncation scheme emerges quite naturally. If, for $m_\mathrm{c} \geqslant 2$, the vertex $\gamma^\Lambda_{m_\mathrm{c}+1}$ on the rhs of the coupled flow equations is replaced by its initial condition $\gamma^{\Lambda_0}_{m_\mathrm{c}+1} = 0$, a closed set of equations for γ_m^Λ with $m \leqslant m_\mathrm{c}$ follows. This set of differential equations can then be integrated over Λ starting at $\Lambda = \Lambda_0$ and going down to $\Lambda = 0$, providing approximate expressions for the γ_m of the original (cut-off free) problem with $m \leqslant m_\mathrm{c}$. Expanding γ_m^Λ in terms of the bare interaction, conventional perturbation theory for the grand canonical potential, the self-energy, the effective interaction, and higher order vertex functions can be recovered from an iterative treatment of the flow equations. It is easy to show that the vertex functions obtained from the truncated equations are at least correct up to order m_c in the bare interaction.

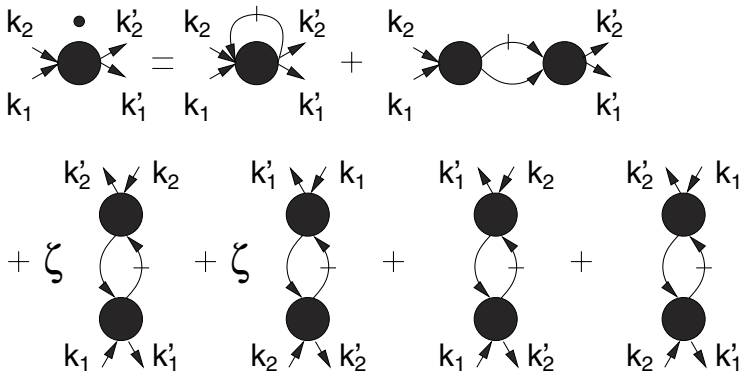

Figure 2. The diagrammatic form of the flow equation for γ_2^Λ. The slashed line stands for the single-scale propagator $\mathcal{S}^\Lambda$ and the unslashed line for $\mathcal{G}^\Lambda$.

To obtain a manageable set of equations in applications of the fRG approach to one- and two-dimensional quantum many-body problems [10–14], further approximations in addition to the above truncation scheme were necessary. In the following two sections we will avoid such additional approximations and solve the truncated fRG equations to order $m_c = 2$ for two zero-dimensional (local) interacting many-particle problems: the quantum harmonic oscillator with a quartic perturbation and the SIAM.

Very recently, a modified version of the flow equation for γ_2^Λ was suggested. As we will consider the truncation order $m_c = 2$, here we only describe this modified scheme for this order. Guided by the idea of an improved fulfilment (compared to the scheme described above) of a certain Ward identity, Katanin replaced the combined propagator $\mathcal{S}^\Lambda$ in the last five terms of equation (21) (the first term does not contribute to order $m_c = 2$) by $-\mathrm{d}\mathcal{G}^\Lambda/\mathrm{d}\Lambda$ [19]. Using

$$\frac{\mathrm{d}\mathcal{G}^\Lambda}{\mathrm{d}\Lambda} = -\mathcal{S}^\Lambda + \mathcal{G}^\Lambda \frac{\mathrm{d}\Sigma^\Lambda}{\mathrm{d}\Lambda}\mathcal{G}^\Lambda$$

obtained from equation (14), it is obvious that the terms added to equation (21) are at least of third order in the bare interaction. Using this modification in the order $m_c = 2$ equations for γ_1^Λ and γ_2^Λ leads to the exact solutions for certain exactly solvable models (reduced BCS model, interacting fermions with forward scattering only). This suggests that the replacement would possibly improve the results from the truncated fRG approach for other models also. In the next section we show that this is indeed the case for the harmonic oscillator with a quartic perturbation. The same holds for the SIAM as discussed in section 4.

3. Application to the anharmonic oscillator

In appropriate units, the Hamiltonian of the harmonic oscillator with a quartic perturbation is given by

$$H = \frac{1}{2}x^2 + \frac{1}{2}p^2 + \frac{g}{4!}x^4, \tag{23}$$

with x the position operator, p the momentum operator, and g the coupling constant. Here we focus on $T = 0$ and are interested in low lying eigenenergies E_n as well as the (imaginary) time ordered propagator

$$\mathcal{G}(\tau) = \langle E_0 | \mathcal{T}\,[x(\tau)x(0)]\,| E_0 \rangle,$$

$|E_n\rangle$ being the eigenstates of the Hamiltonian in equation (23). The Fourier transform of the propagator can be written as

$$\mathcal{G}(\mathrm{i}\omega) = \int_{-\infty}^{\infty} \mathrm{d}\tau\, \mathrm{e}^{\mathrm{i}\omega\tau}\mathcal{G}(\tau) = \frac{1}{\left[\mathcal{G}^0(\mathrm{i}\omega)\right]^{-1} - \Sigma(\mathrm{i}\omega)},$$

where we have introduced the self-energy Σ and the non-interacting propagator

$$\mathcal{G}^0(\mathrm{i}\omega) = \frac{1}{\omega^2 + 1}.$$

In contrast to the more general notation used in the last section, here the propagators and the self-energy depend only on a single frequency and no longer contain the energy conserving δ-function ($T = 0$). The propagator has the Lehmann representation

$$\mathcal{G}(\mathrm{i}\omega) = \frac{1}{2}\sum_{n=1}^{\infty}\left[\frac{1}{\mathrm{i}\omega + (E_n - E_0)} - \frac{1}{\mathrm{i}\omega - (E_n - E_0)}\right]\left|\langle E_0|\,(a + a^\dagger)\,|E_n\rangle\right|^2, \tag{24}$$

where $a, a^\dagger$ denote the usual raising and lowering operators. The spectral weights

$$s_n = \left|\langle E_0|\,(a + a^\dagger)\,|E_n\rangle\right|^2$$

and energies E_n fulfil the f sum rule

$$1 = \sum_{n=1}^{\infty}(E_n - E_0)s_n. \tag{25}$$

It turns out that for the coupling constants $g \leqslant 50$ considered here, the sums in equations (24) and (25) are dominated by the first term. For this reason only the first few eigenstates and eigenenergies are required to obtain accurate ('numerically exact') results for $\mathcal{G}(\mathrm{i}\omega)$. These can quite easily be obtained by expressing H in the basis of eigenstates $|n\rangle$ of the unperturbed harmonic oscillator and numerically diagonalizing the upper left corner of the (infinite) matrix $\langle n|H|n'\rangle$ with $n, n' \leqslant n_\mathrm{c}$ and a sufficiently large n_c. For $g \leqslant 50$, $n_\mathrm{c} = 100$ turns out to be large enough for fulfilling the sum rule (25) to very high precision.

Second-order perturbation theory for the g-dependent part of the ground state energy yields

$$e_0^{(2)} = E_0^{(2)} - E_0^0 = \tfrac{1}{32}g - \tfrac{7}{1536}g^2 \tag{26}$$

and for the self-energy one obtains

$$\Sigma^{(2)}(\mathrm{i}\omega) = -\frac{1}{4}g + \frac{1}{32}g^2 + \frac{1}{8}g^2\frac{1}{\omega^2 + 9}. \tag{27}$$

Within the fRG approach, approximate expressions for

$$E_{n,0} = E_n - E_0$$

and s_n can be obtained from the poles and residues of the propagator $\mathcal{G}(\mathrm{i}\omega)$. Furthermore, since equations (24) and (25) are dominated by the first terms we only consider $E_{1,0}$ and s_1.[3] Second-order approximations for these quantities are given by the smallest pole of $\mathcal{G}^{(2)}(\mathrm{i}\omega) = \left[\omega^2 + 1 - \Sigma^{(2)}(\mathrm{i}\omega)\right]^{-1}$ and the related residue. It is important to note that this approximation $E_{1,0}^{(2)}$ agrees with $E_1^{(2)} - E_0^{(2)}$, where $E_1^{(2)}$ is determined directly from Rayleigh–Schrödinger perturbation theory, only up to second order in g, but is closer to the exact $E_{1,0}$.

[3] For symmetry reasons the s_n with even n vanish. For the g considered here the exact spectral weight s_3 is roughly three orders of magnitude smaller than s_1. Thus extracting more than s_1^{fRG} and $E_{1,0}^{\mathrm{fRG}}$ is beyond the accuracy of our numerical treatment of the flow equations.

Within mean field theory, e_0^{MF} and a frequency independent Σ^{MF} are given by

$$e_0^{\mathrm{MF}} = \frac{1}{2}\sqrt{1+\frac{g}{2}\langle X^2\rangle_{\mathrm{MF}}} - \frac{g}{8}\langle X^2\rangle_{\mathrm{MF}}^2 - \frac{1}{2}, \qquad \Sigma^{\mathrm{MF}} = -\frac{g}{2}\langle X^2\rangle_{\mathrm{MF}}$$

and $\langle X^2\rangle_{\mathrm{MF}}$ is the solution of the self-consistency equation

$$\langle X^2\rangle_{\mathrm{MF}} = \frac{1}{2}\frac{1}{\sqrt{1+g\langle X^2\rangle_{\mathrm{MF}}/2}}.$$

From the mean field propagator one obtains

$$E_{1,0}^{\mathrm{MF}} = \sqrt{1-\Sigma^{\mathrm{MF}}}, \qquad s_1^{\mathrm{MF}} = \frac{1}{2}\frac{1}{\sqrt{1-\Sigma^{\mathrm{MF}}}}.$$

The functional integral representation of the grand canonical partition function of the Hamiltonian equation (23) reads

$$\frac{\mathcal{Z}}{\mathcal{Z}_0} = \frac{1}{\mathcal{Z}_0}\int \mathcal{D}\bar{x}x \exp\left\{(\bar{x}, \left[\mathcal{G}^0\right]^{-1}x)/2 - S_{\mathrm{int}}(\{\bar{x}\},\{x\})\right\}, \tag{28}$$

with

$$S_{\mathrm{int}}(\{\bar{x}\},\{x\}) = \frac{g}{\beta\, 4!}\sum_{n_1,\ldots,n_4}\delta_{n_1+n_2+n_3+n_4,0}\,x(\mathrm{i}\omega_1)x(\mathrm{i}\omega_2)x(\mathrm{i}\omega_3)x(\mathrm{i}\omega_4), \tag{29}$$

$\omega_j = 2\pi n_j/\beta$ bosonic Matsubara frequencies, and $\bar{x}(\mathrm{i}\omega) = x(-\mathrm{i}\omega)$ complex fields. As outlined in the last section and using the frequency cut-off equation (9), flow equations for the γ_m^Λ can be obtained. Here we focus on the equations in truncation order $m_c = 2$. For $T \to 0$ and after introducing

$$e_0^\Lambda = \lim_{T\to 0} T\gamma_0^\Lambda$$

we find

$$\frac{\mathrm{d}}{\mathrm{d}\Lambda}e_0^\Lambda = -\frac{1}{2\pi}\ln[1-\mathcal{G}^0(\mathrm{i}\Lambda)\Sigma^\Lambda(\Lambda)], \tag{30}$$

with the initial condition $e_0^{\Lambda=\infty} = 0$. At the end of the flow, $e_0^{\Lambda=0}$ directly provides the fRG approximation e_0^{fRG} for the g-dependent part of the ground state energy. The flow equation for the self-energy follows as

$$\frac{\mathrm{d}}{\mathrm{d}\Lambda}\Sigma^\Lambda(\mathrm{i}\omega) = \frac{1}{2\pi}\frac{1}{\Lambda^2+1-\Sigma^\Lambda(\mathrm{i}\omega)}g^\Lambda(\mathrm{i}\omega,-\mathrm{i}\omega,\mathrm{i}\Lambda,-\mathrm{i}\Lambda), \tag{31}$$

with the initial condition $\Sigma^{\Lambda=\infty} = 0$ and the fRG approximation for the self-energy $\Sigma^{\mathrm{fRG}}(\mathrm{i}\omega) = \Sigma^{\Lambda=0}(\mathrm{i}\omega)$. Here g^Λ denotes the totally symmetric two-particle vertex which, in contrast to the vertex γ_2^Λ introduced in the last section, does not contain an energy conserving δ-function and factors of β. It depends on only three frequencies, but the fourth will nevertheless always be included in the following. To derive equations (30) and (31) one has to deal with products of delta functions $\delta(|\omega|-\Lambda)$ and terms involving step functions $\Theta(|\omega|-\Lambda)$. These seemingly ambiguous expressions are well defined and unique if the sharp cut-off is implemented as a limit of increasingly sharp broadened cut-off functions Θ_ϵ, with the broadening parameter ϵ tending to zero. The expressions can then be conveniently evaluated by using the following relation [8], valid for arbitrary continuous functions f:

$$\delta_\epsilon(x-\Lambda)f[\Theta_\epsilon(x-\Lambda)] \to \delta(x-\Lambda)\int_0^1 f(t)\,\mathrm{d}t, \tag{32}$$

where $\delta_\epsilon = \mathrm{d}\Theta_\epsilon/\mathrm{d}\epsilon$.

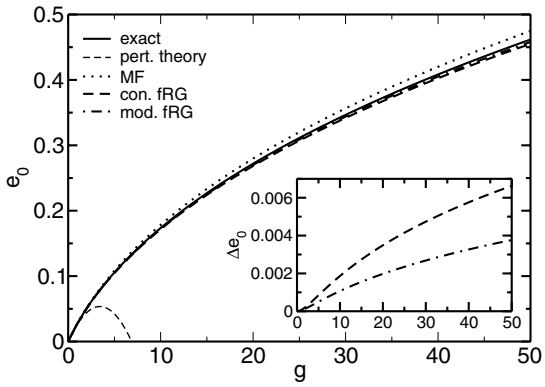

Figure 3. The coupling constant dependent part of the ground state energy $e_0 = E_0 - E_0^0$ as a function of g. Different approximations (second-order perturbation theory (thin dashed curve), mean field theory (dotted curve), the conventional fRG approach (thick dashed curve), the modified fRG approach (dashed–dotted curve)) are compared to the exact result (solid curve). The inset shows the difference between the exact result and the two fRG approximations.

For g^Λ the flow equation reads

$$\begin{aligned}\frac{\mathrm{d}}{\mathrm{d}\Lambda}g^\Lambda(\mathrm{i}\omega_1,\mathrm{i}\omega_2,\mathrm{i}\omega_3,-\mathrm{i}\omega_1-\mathrm{i}\omega_2-\mathrm{i}\omega_3) = \frac{1}{2\pi}\int_{-\infty}^{\infty}\mathrm{d}\nu\,[\mathcal{P}(\mathrm{i}\nu,\mathrm{i}\nu-\mathrm{i}\omega_1-\mathrm{i}\omega_2)\\ \times g^\Lambda(\mathrm{i}\omega_1,\mathrm{i}\omega_2,-\mathrm{i}\nu,\mathrm{i}\nu-\mathrm{i}\omega_1-\mathrm{i}\omega_2)g^\Lambda\\ \times(\mathrm{i}\omega_3,-\mathrm{i}\omega_1-\mathrm{i}\omega_2-\mathrm{i}\omega_3,-\mathrm{i}\nu+\mathrm{i}\omega_1+\mathrm{i}\omega_2,\mathrm{i}\nu)\\ +(\omega_2\leftrightarrow\omega_3)+(\omega_2\leftrightarrow-\omega_1-\omega_2-\omega_3)]\end{aligned} \tag{33}$$

where $\mathcal{P}(\mathrm{i}\nu,\mathrm{i}\nu')$ stands for two different products of propagators. In the conventional fRG scheme it is given by

$$\mathcal{P}_{\mathrm{con}}(\mathrm{i}\nu,\mathrm{i}\nu') = \mathcal{S}^\Lambda(\mathrm{i}\nu)\mathcal{G}^\Lambda(\mathrm{i}\nu') \tag{34}$$

while in the modified scheme [19] one obtains

$$\mathcal{P}_{\mathrm{mod}}(\mathrm{i}\nu,\mathrm{i}\nu') = -\frac{\mathrm{d}\mathcal{G}^\Lambda(\mathrm{i}\nu)}{\mathrm{d}\Lambda}\,\mathcal{G}^\Lambda(\mathrm{i}\nu'). \tag{35}$$

To explicitly evaluate $\mathcal{P}(\mathrm{i}\nu,\mathrm{i}\nu')$, equation (32) has to be used, where special care has to be taken for the case $\nu = \nu'$. In the conventional scheme, $\mathcal{P}_{\mathrm{con}}(\mathrm{i}\nu,\mathrm{i}\nu')$ contains a factor $\delta(|\nu|-\Lambda)$ and the integral over ν in equation (33) can be performed analytically.

To numerically solve the set of differential equations (30), (31), and (33) we have discretized the frequencies (which at $T = 0$ are continuous) on a linear mesh $\omega_j = j\delta$ with $j = -j_0, -j_0+1, \ldots, j_0$.[4] By increasing j_0 and decreasing δ, convergence can be achieved to the required accuracy. For our purposes $j_0 = 40$ and $\delta = 0.5$ turned out to be appropriate. This leads to a set of roughly 5.3×10^5 coupled equations. The Λ integration is started at $\Lambda_0 = 10^5$, making sure that further increasing Λ_0 does not lead to significant changes in the results. Figures 3–5 show comparisons of e_0, $E_{1,0}$, and s_1 with the different approximations considered here (second-order perturbation theory, mean field theory, the conventional fRG approach, the modified fRG approach) and the exact results. Although the approximate fRG

[4] This discretization is not equivalent to considering finite temperatures. Although the fRG method is set up for arbitrary T (see section 2), in most applications calculations were performed at $T = 0$. fRG results for finite T, obtained using a smooth frequency cut-off, for the problem of resonant tunnelling in a Luttinger liquid are presented in [20].

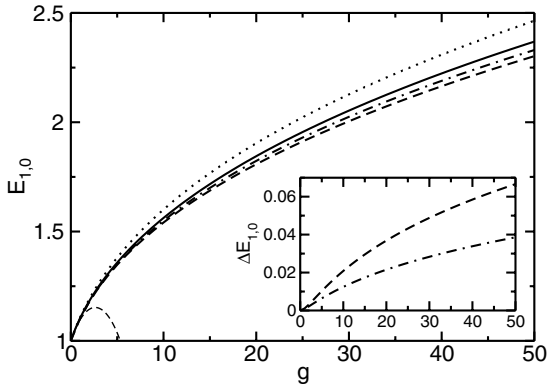

Figure 4. As figure 3, but for the energy difference $E_{1,0}$ of the first excited state and the ground state.

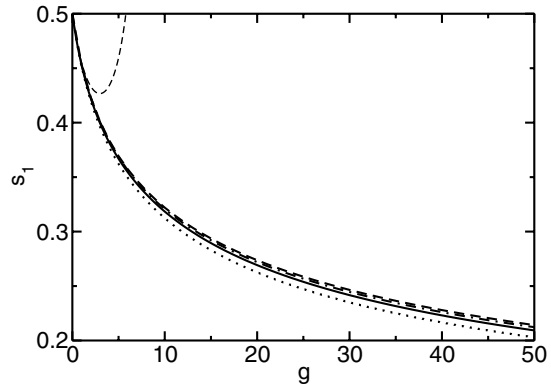

Figure 5. As figure 3, but for the spectral weight s_1 of the first peak.

approaches correctly reproduce only the first two derivatives with respect to g at $g = 0$, they give extremely accurate results even up to $g = 50$, while conventional second-order perturbation theory can only be trusted for $g < 1$. This provides an impressive example of the power of 'renormalization group enhanced perturbation theory'. Comparing the two fRG approximations, the modified scheme is roughly a factor of two closer to the exact result and thus a substantial improvement [19][5].

To avoid the problem of analytic continuation (see the next section), the results for $e_{1,0}^{\mathrm{fRG}}$ and s_1^{fRG} were obtained by fitting a function $a/(\omega^2 + b^2)$ with a and b as fitting parameters to $\mathcal{G}^{\mathrm{fRG}}(\mathrm{i}\omega) = [\omega^2 + 1 - \Sigma^{\mathrm{fRG}}(\mathrm{i}\omega)]^{-1}$. Assuming this fitting form, we have used that the spectral function is dominated by the first peak (see footnote 4). For the problem studied, mean field theory also leads to fairly accurate results (but not as good as the fRG ones). This is related to the fact that low lying eigenstates of the Hamiltonian in equation (23) can be described quite well by the eigenstates of a harmonic oscillator with a shifted frequency determined self-consistently.

[5] For the classical anharmonic oscillator also, compared to the conventional scheme the modified fRG approach [19] leads to better agreement with the exact result.

4. Single-particle dynamics of the single-impurity Anderson model

In contrast to the anharmonic oscillator studied in the previous section, the single-impurity Anderson model [21]

$$H = \sum_{\vec{k}\sigma} \epsilon_{\vec{k}} c^{\dagger}_{\vec{k}\sigma} c_{\vec{k}\sigma} + \epsilon_d \sum_{\sigma} d^{\dagger}_{\sigma} d_{\sigma} + U d^{\dagger}_{\uparrow} d_{\uparrow} d^{\dagger}_{\downarrow} d_{\downarrow} + \frac{V}{\sqrt{N}} \sum_{\vec{k}\sigma} \left(c^{\dagger}_{\vec{k}\sigma} d_{\sigma} + \text{h.c.} \right) \quad (36)$$

consists of two subsystems, namely a 'conduction band' with a continuous energy spectrum described by the first term in equation (36) and a localized level (typically referred to as the 'd' state) with energy ϵ_{d} relative to the chemical potential μ of the conduction electrons. Two electrons occupying the localized level are in addition subject to a Coulomb repulsion $U > 0$. The two subsystems are coupled via the hybridization in the last term. As the two-body interaction is restricted to a single level, the SIAM falls into the class of zero-dimensional interacting systems.

While this model looks rather simple, it contains all the ingredients to make it a complicated many-body problem. The bare energy scales of the model are the bandwidth W of the band electrons, the local energy ϵ_{d}, the Coulomb repulsion U, and the bare level width generated by the hybridization, $\Delta_0 = \pi V^2 \rho_{\mathrm{c}}(\mu)$, where $\rho_{\mathrm{c}}(\epsilon)$ denotes the density of states of the conduction states which is assumed to be slowly varying. In the following we restrict ourselves to the particle–hole symmetric case $2\epsilon_{\mathrm{d}} + U = 2\mu = 0$. As in the parameter regime $U/\Delta_0 \gg 1$ the charge fluctuations on the d level from the average value 1 are small, this system can be effectively described as a spin antiferromagnetically coupled to the conduction electron spin density [22]: the so-called Kondo model [23]. This antiferromagnetic coupling leads to a screening of the local spin by the conduction electrons with a characteristic energy scale $\ln(T_{\mathrm{K}}) \propto -1/\Delta_0$, the Kondo temperature. As is apparent from this expression, T_{K} depends non-analytically on Δ_0, signalling the occurrence of infrared divergences in perturbation theories in Δ_0/U [24] and a severe problem for computational techniques, namely the task of resolving an exponentially small energy scale.

On the other hand, the physics in the regimes $T, \omega \gg T_{\mathrm{K}}$ and $T, \omega \ll T_{\mathrm{K}}$ is comparatively simple. For $T, \omega \gg T_{\mathrm{K}}$ it is governed by charge excitations with energies ϵ_{d} and $\epsilon_{\mathrm{d}} + U$ with a lifetime given by $1/(2\Delta_0)$. In the other limit $T, \omega \ll T_{\mathrm{K}}$, it has been worked out using Wilson's NRG [25] that the system can again be described by a Hamiltonian of the form equation (36), but with $U \to U^* = 0$, $\epsilon_{\mathrm{d}} \to \epsilon^*_{\mathrm{d}} = 0$, and Δ_0 replaced by $\Delta^*_0 \sim T_{\mathrm{K}}$. This regime has been termed a 'local Fermi liquid' by Nozières [24]. This effective description yields a narrow resonance at the chemical potential in the spectral function of the d Green function which in the symmetric case takes the form

$$G_{\mathrm{dd}}(\mathrm{i}\nu) = \frac{1}{\mathrm{i}\nu - \Delta(\mathrm{i}\nu) - \tilde{\Sigma}(\mathrm{i}\nu)}. \quad (37)$$

Here $\Delta(\mathrm{i}\nu) = V^2 \int \mathrm{d}\epsilon\, \rho_{\mathrm{c}}(\epsilon)/(\mathrm{i}\nu - \epsilon)$ and $\tilde{\Sigma}$ denotes all self-energy contributions of second and higher order in U. As a special feature of the symmetric case, the approximation of only keeping the second-order self-energy $\Sigma^{(2)}$ already describes the qualitative behaviour of the d spectral function for different values of U/Δ_0 correctly [24]. For $U/\Delta_0 \ll 1$ there is a Lorentzian peak at the chemical potential with a width differing little from Δ_0. For $U/\Delta_0 \gg 1$ most of the spectral weight is in the high energy peaks near $\pm U/2$ with a narrow resonance at $\mu = 0$. Quantitatively, the width and shape of this Kondo (or Abrikosov–Suhl) resonance are described poorly using $\Sigma^{(2)}$ vanishing only with Δ_0/U. From the results of section 3 one expects the application of the functional renormalization group approach to the SIAM to lead to improvements over the direct perturbational description of the Kondo resonance.

For the SIAM the fRG results can be compared to the outcome of NRG calculations [1, 25]. An important aspect of the treatment of the SIAM with the fRG approach is that, while the numerical effort of the NRG method increases exponentially with the number of impurity degrees of freedom, e.g. in the case of additional orbital degrees of freedom or for a system of many magnetic impurities, the increase in computational resources necessary in the fRG approach described below is governed by at most a power law.

The starting point of our fRG approach is again equations (19) and (21). We also use $m_c = 2$; i.e. we replace the three-particle vertex by its initial condition $\gamma_3^\Lambda = 0$, and consider $T = 0$ only. We again use the frequency cut-off described in equation (9) and, because we concentrate here on spectral properties, only flow equations for the self-energy and for the two-particle vertex (and not the ground state energy) will be derived. Note that calculation of two-particle properties is possible within the same scheme without further difficulties [11] and will be discussed in a forthcoming publication.

For the SIAM all Green functions $G_{i,j}$ different from G_{dd} can be expressed in terms of G_{dd} and Green functions of the non-interacting system. For the calculation of G_{dd} the index k is replaced by a spin index σ and a frequency ν. The two-particle vertex can then be written as

$$\gamma_2^\Lambda(k_1', k_2'; k_1, k_2) = \delta(\nu_1 + \nu_2 - \nu_1' - \nu_2') \times \{\delta_{\sigma_1,\sigma_1'}\delta_{\sigma_2,\sigma_2'}\mathcal{U}^\Lambda(\mathrm{i}\nu_1', \mathrm{i}\nu_2'; \mathrm{i}\nu_1, \mathrm{i}\nu_2) - \delta_{\sigma_1,\sigma_2'}\delta_{\sigma_2,\sigma_1'}\mathcal{U}^\Lambda(\mathrm{i}\nu_2', \mathrm{i}\nu_1'; \mathrm{i}\nu_1, \mathrm{i}\nu_2)\}. \quad (38)$$

This can be used to perform the sum over the spins in equation (19) and we find for the self-energy

$$\frac{\mathrm{d}}{\mathrm{d}\Lambda}\Sigma^\Lambda(\mathrm{i}\nu) = -\frac{1}{2\pi}\int_{-\infty}^{\infty}\mathrm{d}\nu'\,\mathcal{S}^\Lambda(\mathrm{i}\nu')[2\mathcal{U}^\Lambda(\mathrm{i}\nu, \mathrm{i}\nu'; \mathrm{i}\nu, \mathrm{i}\nu') - \mathcal{U}^\Lambda(\mathrm{i}\nu', \mathrm{i}\nu; \mathrm{i}\nu, \mathrm{i}\nu')]. \quad (39)$$

In order to derive a flow equation for $\mathcal{U}^\Lambda(\mathrm{i}\nu_1', \mathrm{i}\nu_2'; \mathrm{i}\nu_1, \mathrm{i}\nu_2)$, with $\nu_2 = \nu_1' + \nu_2' - \nu_1$, the spin sum in equation (21) has to be performed as well. This leads to the lengthy expression (A.1), presented in the appendix.

The initial values are given by $\Sigma^{\Lambda=\infty}(\mathrm{i}\nu) = 0$ and $\mathcal{U}^{\Lambda=\infty}(\mathrm{i}\nu_1', \mathrm{i}\nu_2'; \mathrm{i}\nu_1, \mathrm{i}\nu_2) = U$. In the numerical solution of these flow equations we start integrating at finite $\Lambda_0 \gg \max(U, \Delta_0)$. The integration from $\Lambda = \infty$ to Λ_0 can be performed analytically. Up to corrections of order Λ_0^{-1} the new initial conditions are $\Sigma^{\Lambda_0}(\mathrm{i}\nu) = U/2$ and $\mathcal{U}^{\Lambda_0}(\mathrm{i}\nu_1', \mathrm{i}\nu_2'; \mathrm{i}\nu_1, \mathrm{i}\nu_2) = U$.

$\mathcal{S}^\Lambda(\mathrm{i}\nu)$ and $\mathcal{P}^\Lambda_{\mathrm{con}}(\mathrm{i}\nu, \mathrm{i}\nu') = \mathcal{S}^\Lambda(\mathrm{i}\nu)\mathcal{G}^\Lambda(\mathrm{i}\nu')$ are calculated in the same way as for the anharmonic oscillator using equation (32), and are given by

$$\mathcal{S}^\Lambda(\mathrm{i}\nu) \to \delta(|\nu| - \Lambda)\frac{1}{\left[\mathcal{G}^0(\mathrm{i}\nu)\right]^{-1} - \Sigma^\Lambda(\mathrm{i}\nu)}, \quad (40)$$

with $[\mathcal{G}^0(\mathrm{i}\nu)]^{-1} = \mathrm{i}\nu - \Delta(\mathrm{i}\nu) - \epsilon_d$ and

$$\mathcal{P}^\Lambda_{\mathrm{con}}(\mathrm{i}\nu, \mathrm{i}\nu') \to \delta(|\nu| - \Lambda)\frac{1}{\left[\mathcal{G}^0(\mathrm{i}\nu)\right]^{-1} - \Sigma^\Lambda(\mathrm{i}\nu)}\frac{\Theta(|\nu'| - \Lambda)}{\left[\mathcal{G}^0(\mathrm{i}\nu')\right]^{-1} - \Sigma^\Lambda(\mathrm{i}\nu')} \quad (41)$$

with $\Theta(0) = 1/2$. In our calculations we use the limit of an infinite bandwidth, i.e. $\Delta(\mathrm{i}\nu) \to -\mathrm{i}\,\mathrm{sgn}(\nu)\Delta_0$. The results from second-order perturbation theory for the self-energy can be recovered by replacing the self-energy on the rhs of equations (39) and (A.1) and $\mathcal{U}^\Lambda$ on the rhs of equation (A.1) by their initial values. It turns out that the fRG version using $\mathcal{P}^\Lambda_{\mathrm{con}}$ gives good results for $U/\Delta_0 < 3$, but fails to provide the expected improvement compared to the use of $\Sigma^{(2)}$ for $U/\Delta_0 > 3$. This will be discussed in more detail in a forthcoming publication. For this reason we follow [19] and replace $\mathcal{P}^\Lambda_{\mathrm{con}}(\mathrm{i}\nu, \mathrm{i}\nu')$ by $\mathcal{P}^\Lambda_{\mathrm{mod}}(\mathrm{i}\nu, \mathrm{i}\nu') = -\mathcal{G}^\Lambda(\mathrm{i}\nu')\frac{\mathrm{d}}{\mathrm{d}\Lambda}\mathcal{G}^\Lambda(\mathrm{i}\nu)$ in equation (A.1). Applying equation (32) yields

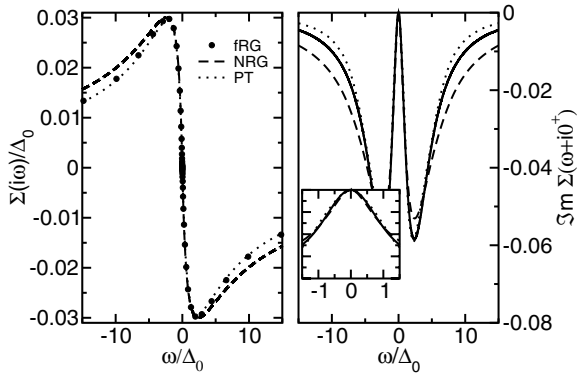

Figure 6. Left panel: $\Sigma(\mathrm{i}\omega)$ from the fRG approach for $U = \Delta_0$ (circles) compared to the NRG (dashed curve) and second-order perturbation theory (dotted curve) results. Right panel: $\mathrm{Im}\,\Sigma(\omega + \mathrm{i}0^+)$ for the fRG approach obtained from Padé approximants for the data in the left panel. The inset shows an enlarged view around $\omega = 0$.

$$-\mathcal{G}^{\Lambda}(\mathrm{i}\nu')\frac{\mathrm{d}}{\mathrm{d}\Lambda}\mathcal{G}^{\Lambda}(\mathrm{i}\nu) \to \delta(|\nu| - \Lambda)\frac{1}{[\mathcal{G}^0(\mathrm{i}\nu)]^{-1} - \Sigma^{\Lambda}(\mathrm{i}\nu)}\frac{\Theta(|\nu'| - \Lambda)}{[\mathcal{G}^0(\mathrm{i}\nu')]^{-1} - \Sigma^{\Lambda}(\mathrm{i}\nu')} - \frac{\mathrm{d}}{\mathrm{d}\Lambda}\Sigma^{\Lambda}(\mathrm{i}\nu)\,\frac{\Theta(|\nu| - \Lambda)}{[[\mathcal{G}^0(\mathrm{i}\nu)]^{-1} - \Sigma^{\Lambda}(\mathrm{i}\nu)]^2}\frac{\Theta(|\nu'| - \Lambda)}{[\mathcal{G}^0(\mathrm{i}\nu')]^{-1} - \Sigma^{\Lambda}(\mathrm{i}\nu')}. \tag{42}$$

For the integration of the $T = 0$ flow equations, the continuous frequencies again have to be discretized. However, in contrast to the anharmonic oscillator case it is not sufficient to work with a linear mesh. Because for $U/\Delta_0 \gg 1$ the Kondo resonance is visible only on an exponentially small energy scale around the Fermi level, we use a combination of a linear and a logarithmic mesh. This enables us to recover both the high energy and the low energy physics, keeping the number of frequencies to a manageable size. The numerical effort grows with the third power of the number of frequencies in the conventional version and with almost the fourth power using the modified version, due to the absence of a δ-function in the last term of equation (42).

In the fRG approach one naturally obtains the self-energy for imaginary frequencies. In order to calculate spectral functions, an analytic continuation to the real axis is necessary, which is known to be an ill-posed problem. Since the results from the fRG approach are not subject to statistical errors or noise, like for example quantum Monte Carlo data, we have applied the method of Padé approximation [26] to obtain $\Sigma(z)$ from $\Sigma(\mathrm{i}\nu)$. We find that especially the low-energy part of the spectral function which contains the Kondo resonance can be reliably extracted if sufficiently many frequencies close to the Fermi level are used (see below).

As an example, we present in figure 6 the calculated $\Sigma(\mathrm{i}\omega)$ (left panel) and the corresponding $\mathrm{Im}\,\Sigma(\omega + \mathrm{i}0^+)$ from the Padé approximation (right panel) for $U/\Delta_0 = 1$. The dashed and dotted curves represent results from the NRG approach and second-order perturbation theory, respectively. The inset in the right panel shows an enlarged view of the region around $\omega = 0$. For such small U/Δ_0, second-order perturbation theory provides accurate results for all relevant energy scales. On low energy scales this can be seen from a comparison with very accurate NRG results, e.g. those presented in the right panel of figure 6. For higher energies the accuracy of second-order perturbation theory has already been established in a comparison to the local moment approach [27]. Thus, the discrepancies for large ω between the fRG approach and second-order perturbation theory on the one hand and

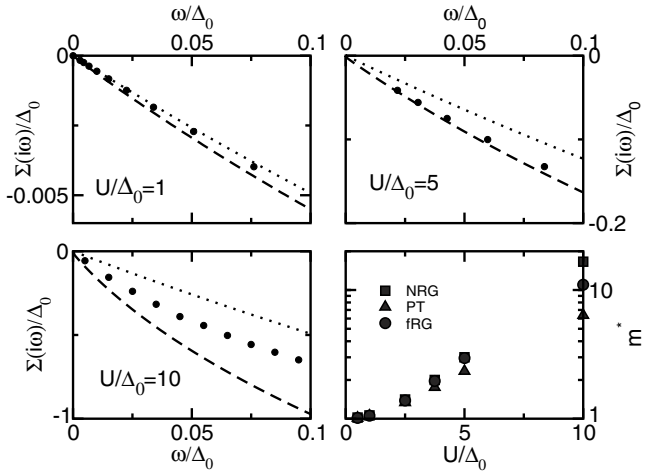

Figure 7. $\Sigma(\mathrm{i}\omega)$ from the fRG approach (circles) for $U/\Delta_0 = 1$, 5, and 10 compared to NRG (dashed curve) and second-order perturbation theory (dotted curve) results. Bottom right: the effective mass m^* from the fRG approach (circles), the NRG approach (squares), and second-order perturbation theory (triangles).

NRG on the other must be attributed to well known broadening effects in the NRG approach. Apparently, the Padé approximation to the fRG provides reliable results, in particular around $\omega = 0$, and recovers the perturbation theory as expected for such a small value of U/Δ_0.

The true test for the method however is a comparison of the self-energy to NRG results for larger values of U and, in particular, the behaviour on low energy scales. Such a comparison is presented in figure 7 for $U/\Delta_0 = 1$, 5, and 10. For $U/\Delta_0 = 5$ the fRG results are still in excellent agreement with the NRG data, while second-order perturbation theory already deviates. For $U = 10\Delta_0$ we observe a significant dependence of the general structures, in particular the Hubbard bands at $\omega \approx \pm U/2$, and also of the slope at $\omega \to 0$ on details of the discretization mesh. It seems necessary to have an extremely fine resolution around $\omega \to 0$ and a sufficient resolution around $\omega \approx \pm U/2$. With an exponentially vanishing low energy scale these constraints are hard to fulfil with both linear and logarithmic meshes keeping the number of flow equations to a manageable size. The bottom left panel contains the best fRG data we have been able to obtain so far. A more extended discussion of this issue will be presented in a forthcoming publication.

In addition to the self-energy, the effective mass m^* obtained from

$$m^* = 1 + \lim_{\omega \searrow 0} \frac{\mathrm{Im}\,\Sigma(\mathrm{i}\omega)}{\omega}$$

as a function of U is depicted, in the bottom right panel of figure 7. This quantity is directly related to the Kondo temperature [24]. Compared to that in perturbation theory, the effective mass is much closer to the very accurate values determined from the NRG approach.

The evolution of the spectral function of the d level, $\rho_{\mathrm{d}}(\omega) = -\frac{1}{\pi}\,\mathrm{Im}\,G_{\mathrm{d}}(\omega + \mathrm{i}0^+)$ for the above values of U is assembled in figure 8. The inset shows a comparison to NRG and perturbation theory results for the region around $\omega = 0$ at $U/\Delta_0 = 10$. One can see very nicely the development of the sharp resonance in the spectrum and the formation of the Hubbard bands with increasing U. Due to the insufficient resolution at larger ω in the calculation for $U/\Delta_0 = 10$, the Hubbard bands come out too broad here. We believe that an improved discretization of the energy mesh in the solution of the flow equations will remedy

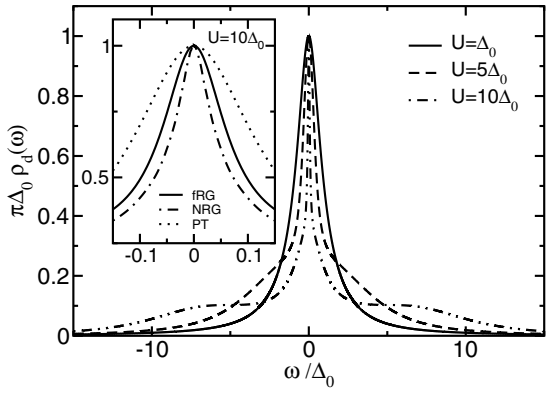

Figure 8. The evolution of the fRG spectral function for the d level for the values of U in figure 7. The inset shows a comparison to NRG results for $U/\Delta_0 = 10$ for the region around $\omega = 0$.

that particular problem. The important region around $\omega = 0$ on the other hand is captured rather well by the fRG approach. It is in particular noteworthy that the functional form at low frequencies (see the inset) apparently does not follow a Lorentzian but rather, like the NRG form, the more complex scaling form with logarithmic tails predicted by Logan *et al* [28].

5. Summary and outlook

We have presented an application of the functional renormalization group technique to solve for the dynamics of zero-dimensional interacting quantum problems. We discussed, as particular examples, the anharmonic oscillator and the single-impurity Anderson model. In both cases the fRG approach proved to be a substantial improvement over conventional low order perturbation theory and to give results rather close to the very accurate ones obtained numerically.

We also investigated the differences between the conventional fRG approach and a modification suggested by Katanin [19], which should improve the accuracy of the method further. That this is indeed true was shown directly for the anharmonic oscillator. For the single-impurity Anderson model it was actually necessary to use this modified version to obtain sensible results for values $U/\Delta_0 > 3$.

An important aspect of the fRG approach is that extension of the SIAM to more complex systems, such as orbital degrees of freedom or systems of coupled impurities, is straightforward. This is in principle also true for Wilson's NRG approach. In the latter, however, the exponentially increasing Hilbert space quickly renders a practical application impossible. For the fRG approach, on the other hand, the major modification will be an increase in the number of equations, which means that the numerical effort will increase at most following a power law. This feature makes the fRG approach a possible method for studying features of complex impurity systems and, in particular, a potential 'impurity solver' for mean field theories of interacting lattice models such as the Hubbard model in the framework of the dynamical mean field theory [29] or the dynamical cluster approximation [30]. Furthermore, as becomes clear from considering the anharmonic oscillator, the fRG approach is of equal complexity for bosonic and fermionic systems. This opens the possibility of studying combinations of such degrees of freedom in impurity models. A question which can be addressed using the fRG approach is the influence of phonons or magnetic fluctuations on low energy scales. Within the dynamical mean field theory the metal–insulator transition in the presence of phonons (Kondo

volume collapse [31]) as well as the problem of non-Fermi liquid formation in for example $CeCu_{6-x}Au_x$ [32] can be studied.

Acknowledgments

We thank S Dusuel, W Metzner, M Salmhofer, H Schoeller, and G Uhrig for useful discussions. This work was supported by the SFB 602 of the Deutsche Forschungsgemeinschaft (RH and KS). VM is grateful to the Bundesministerium für Bildung und Forschung for support.

Appendix

Depending on the specific parametrization of the two-particle vertex, flow equations for the relevant frequency dependent parts of the vertex and for the self-energy can be derived by using the spin conservation on the vertex when the sum over spins in equation (21) is performed. For the form of the vertex given in equation (38) the corresponding flow equation for the self-energy is given by equation (39), and the equation for the frequency dependent part of the vertex $\mathcal{U}^\Lambda(i\nu_1', i\nu_2'; \nu_1, i\nu_2)$ with $\nu_2 = \nu_1' + \nu_2' - \nu_1$ reads

$$\begin{aligned}\frac{d}{d\Lambda}\mathcal{U}^\Lambda(i\nu_1', i\nu_2'; i\nu_1, i\nu_2) = -\frac{1}{2\pi}\int_{-\infty}^{\infty} d\nu[&\mathcal{P}^\Lambda(i\nu, i\nu_1 + i\nu_2 - i\nu)\\
&\times(-\mathcal{U}^\Lambda(i\nu, i\nu_1 + i\nu_2 - i\nu; i\nu_1, i\nu_2)\mathcal{U}^\Lambda(i\nu_2', i\nu_1'; i\nu_1 + i\nu_2 - i\nu, i\nu)\\
&- \mathcal{U}^\Lambda(i\nu_1 + i\nu_2 - i\nu, i\nu; i\nu_1, i\nu_2)\mathcal{U}^\Lambda(i\nu_1', i\nu_2'; i\nu_1 + i\nu_2 - i\nu, i\nu))\\
&+ \{\mathcal{P}^\Lambda(i\nu, -i\nu_1 + i\nu_1' + i\nu)\\
&\times(2\mathcal{U}^\Lambda(i\nu_1', i\nu; i\nu_1, -i\nu_1 + i\nu_1' + i\nu)\mathcal{U}^\Lambda(i\nu_2', -i\nu_1 + i\nu_1' + i\nu; i\nu_2, i\nu)\\
&- \mathcal{U}^\Lambda(i\nu_1', i\nu; i\nu_1, -i\nu_1 + i\nu_1' + i\nu)\mathcal{U}^\Lambda(-i\nu_1 + i\nu_1' + i\nu, i\nu_2'; i\nu_2, i\nu)\\
&- \mathcal{U}^\Lambda(i\nu, i\nu_1'; i\nu_1, -i\nu_1 + i\nu_1' + i\nu)\mathcal{U}^\Lambda(i\nu_2', -i\nu_1 + i\nu_1' + i\nu; i\nu_2, i\nu))\\
&+ (1' \leftrightarrow 2'; 1 \leftrightarrow 2)\}\\
&- \{\mathcal{P}^\Lambda(i\nu, -i\nu_1 + i\nu_2' + i\nu)\\
&\times\mathcal{U}^\Lambda(i\nu, i\nu_2'; i\nu_1, -i\nu_1 + i\nu_2' + i\nu)\mathcal{U}^\Lambda(-i\nu_1 + i\nu_2' + i\nu, i\nu_1'; i\nu_2, i\nu)\\
&+ (1' \leftrightarrow 2'; 1 \leftrightarrow 2)\}].\end{aligned} \tag{A.1}$$

Again $\mathcal{P}$ stands either for $\mathcal{P}_{con}$ or for $\mathcal{P}_{mod}$.

Two other possible parametrizations of the two-particle vertex are

$$\begin{aligned}\gamma_2^\Lambda(k_1', k_2'; k_1, k_2) = \delta(\nu_1 + \nu_2 - \nu_1' - \nu_2')\{&\delta_{\sigma_1,\sigma_2}\delta_{\sigma_1',\sigma_2'}\delta_{\sigma_1,\sigma_1'}\mathcal{U}_p^\Lambda(i\nu_1', i\nu_2'; i\nu_1, i\nu_2)\\
&+ \delta_{\sigma_1,-\sigma_2}\delta_{\sigma_1',-\sigma_2'}(\delta_{\sigma_1,\sigma_1'}\mathcal{U}_a^\Lambda(i\nu_1', i\nu_2'; i\nu_1, i\nu_2) - \delta_{\sigma_1,-\sigma_1'}\mathcal{U}_a^\Lambda(i\nu_2', i\nu_1'; i\nu_1, i\nu_2))\}\end{aligned}$$

and

$$\begin{aligned}\gamma_2^\Lambda(k_1', k_2'; k_1, k_2) = \delta(\nu_1 + \nu_2 - \nu_1' - \nu_2')\{&S_{\sigma_1',\sigma_2';\sigma_1,\sigma_2}\mathcal{U}_S^\Lambda(i\nu_1', i\nu_2'; i\nu_1, i\nu_2)\\
&+ T_{\sigma_1',\sigma_2';\sigma_1,\sigma_2}\mathcal{U}_T^\Lambda(i\nu_1', i\nu_2'; i\nu_1, i\nu_2)\}\end{aligned}$$

with

$$S_{\sigma_1',\sigma_2';\sigma_1,\sigma_2} = \tfrac{1}{2}\left(\delta_{\sigma_1,\sigma_1'}\delta_{\sigma_2,\sigma_2'} - \delta_{\sigma_1,\sigma_2'}\delta_{\sigma_2,\sigma_2'}\right);\ T_{\sigma_1',\sigma_2';\sigma_1,\sigma_2} = \tfrac{1}{2}\left(\delta_{\sigma_1,\sigma_1'}\delta_{\sigma_2,\sigma_2'} + \delta_{\sigma_1,\sigma_2'}\delta_{\sigma_2,\sigma_2'}\right).$$

These two parametrizations lead to different sets of flow equations for the self-energy and to two sets of flow equations for the frequency dependent functions $\mathcal{U}_p^\Lambda$ and $\mathcal{U}_a^\Lambda$ for the first case and $\mathcal{U}_S^\Lambda$ and $\mathcal{U}_T^\Lambda$ for the second case (compared to one set for the parametrization equation (38)),

implying an increased numerical effort. They are useful for investigating further the processes occurring during the integration of the flow equations; in this way we are able to distinguish between the behaviours of different channels of the interaction.

References

[1] Wilson K G 1975 *Rev. Mod. Phys.* **47** 773
[2] Glazek S D and Wiegmann P B 1993 *Phys. Rev.* D **48** 5863
Wegner F 1994 *Ann. Phys., Lpz.* **3** 77
[3] Lenz P and Wegner F 1996 *Nucl. Phys.* B **482** 693
Mielke A 1997 *Europhys. Lett.* **40** 195
Ragwitz M and Wegner F 1999 *Eur. Phys. J.* B **8** 9
[4] Uhrig G S 1998 *Phys. Rev.* B **57** R14004
Knetter C and Uhrig G S 2000 *Eur. Phys. J.* B **13** 209
[5] Kehrein S and Mielke A 1996 *Ann. Phys.* **252** 1
Slezak C, Kehrein S, Pruschke Th and Jarrell M 2003 *Phys. Rev.* B **67** 184408
[6] Polchinski J 1984 *Nucl. Phys.* B **231** 269
[7] Wetterich C 1993 *Phys. Lett.* B **301** 90
[8] Morris T R 1994 *Int. J. Mod. Phys.* A **9** 2411
[9] Salmhofer M 1998 *Renormalization* (Berlin: Springer)
[10] Zanchi D and Schulz H J 2000 *Phys. Rev.* B **61** 13609
[11] Halboth C J and Metzner W 2000 *Phys. Rev.* B **61** 7364
[12] Honerkamp C, Salmhofer M, Furukawa N and Rice T M 2001 *Phys. Rev.* B **63** 035109
[13] Busche T, Bartosch L and Kopietz P 2002 *J. Phys.: Condens. Matter* **14** 8513
[14] Meden V, Metzner W, Schollwöck U and Schönhammer K 2002 *Phys. Rev.* B **65** 045318
Meden V, Metzner W, Schollwöck U and Schönhammer K 2002 *J. Low Temp. Phys.* **126** 1147
Andergassen S, Enss T, Meden V, Metzner W, Schollwöck U and Schönhammer K 2004 *Phys. Rev.* B at press
(Andergassen S, Enss T, Meden V, Metzner W, Schollwöck U and Schönhammer K 2004 *Preprint* cond-mat/0403517)
[15] Honerkamp C and Salmhofer M 2003 *Phys. Rev.* B **67** 174504
[16] For e.g., see, Bender C M and Wu T T 1969 *Phys. Rev.* **184** 1231
Bender C M and Wu T T 1971 *Phys. Rev. Lett.* **27** 461
Janke W and Kleinert H 1995 *Phys. Rev. Lett.* **75** 2787
Weniger E J 1996 *Phys. Rev. Lett.* **77** 2859
Bender C M and Bettencourt L M A 1996 *Phys. Rev. Lett.* **77** 4114
Hatsuda T, Kunihiro T and Tanaka T 1997 *Phys. Rev. Lett.* **78** 3229
Meurice Y 2002 *Phys. Rev. Lett.* **88** 141601 and references therein
[17] Dusuel S and Uhrig G 2004 *Preprint* cond-mat/0405166
[18] Negele J W and Orland H 1988 *Quantum Many-Particle Physics* (New York: Addison-Wesley)
[19] Katanin A A 2004 *Preprint* cond-mat/0402602
[20] Meden V, Enss T, Andergassen S, Metzner W and Schönhammer K 2004 *Preprint* cond-mat/0403655
[21] Anderson P W 1961 *Phys. Rev.* **124** 41
[22] Schrieffer R and Wolff P A 1966 *Phys. Rev.* **149** 491
[23] Kondo J 1964 *Prog. Theor. Phys.* **32** 37
[24] Hewson A C 1993 *The Kondo Problem to Heavy Fermions* ed D Edwards and D Melville (Cambridge: Cambridge University Press)
[25] Krishnamurthy H R, Wilkins J W and Wilson K G 1980 *Phys. Rev.* B **21** 1003
[26] Press W H *et al* 1993 *Numerical Recipes in C* (Cambridge: Cambridge University Press)
[27] Logan D, Eastwood M and Tusch M 1998 *J. Phys.: Condens. Matter* **10** 2673
[28] Logan D and Glossop M 2000 *J. Phys.: Condens. Matter* **12** 985
[29] Pruschke Th, Jarrell M and Freericks J K 1995 *Adv. Phys.* **44** 187
Georges A, Kotliar G, Krauth W and Rozenberg M J 1996 *Rev. Mod. Phys.* **68** 13
[30] Maier Th, Jarrell M, Pruschke Th and Hettler M 2004 *Preprint* cond-mat/0404055
[31] Allen J W and Martin R M 1982 *Phys. Rev. Lett.* **49** 1106
Allen J W and Liu L Z 1992 *Phys. Rev.* B **46** 5047
Lavagna M *et al* 1982 *Phys. Lett.* A **90** 210
[32] Smith J L and Si Q 2000 *Phys. Rev.* B **61** 5184